Structural Determinants for Functional Coupling Between the β and α Subunits in the Ca^{2+}-activated K^+ (BK) Channel

Patricio Orio,[1] Yolima Torres,[1,2] Patricio Rojas,[1,3] Ingrid Carvacho,[1,4] Maria L. Garcia,[5] Ligia Toro,[6] Miguel A. Valverde,[7] and Ramon Latorre[1,3]

[1]Department of Biophysics and Molecular Physiology, Centro de Estudios Científicos, Valdivia 5110246, Chile
[2]Universidad del Valle, Cali, Colombia
[3]Facultad de Ciencias, Universidad de Chile, Santiago 7800024, Chile
[4]Universidad Austral de Chile, Valdivia, Chile
[5]Department of Ion Channels, Merck Research Laboratories, Rahway, NJ 07065
[6]Department of Anesthesiology University of California, Los Angeles, CA 90095
[7]Grup de Canalopaties, Unitat de Senyalització Celular, Universitat Pompeu Fabra, Barcelona 08003, Spain

High conductance, calcium- and voltage-activated potassium (BK, MaxiK) channels are widely expressed in mammals. In some tissues, the biophysical properties of BK channels are highly affected by coexpression of regulatory (β) subunits. The most remarkable effects of β1 and β2 subunits are an increase of the calcium sensitivity and the slow down of channel kinetics. However, the detailed characteristics of channels formed by α and β1 or β2 are dissimilar, the most remarkable difference being a reduction of the voltage sensitivity in the presence of β1 but not β2. Here we reveal the molecular regions in these β subunits that determine their differential functional coupling with the pore-forming α-subunit. We made chimeric constructs between β1 and β2 subunits, and BK channels formed by α and chimeric β subunits were expressed in *Xenopus laevis* oocytes. The electrophysiological characteristics of the resulting channels were determined using the patch clamp technique. Chimeric exchange of the different regions of the β1 and β2 subunits demonstrates that the NH_3 and COOH termini are the most relevant regions in defining the behavior of either subunit. This strongly suggests that the intracellular domains are crucial for the fine tuning of the effects of these β subunits. Moreover, the intracellular domains of β1 are responsible for the reduction of the BK channel voltage dependence. This agrees with previous studies that suggested the intracellular regions of the α-subunit to be the target of the modulation by the β1-subunit.

The Journal of General Physiology

INTRODUCTION

Large conductance Ca^{2+}-activated K^+ (BK, MaxiK) channels are ubiquitously distributed in different cells and tissues. One of their roles is to dampen excitatory signals induced by increases in cytoplasmic Ca^{2+} concentration and/or membrane depolarization (Meech, 1978; McManus and Magleby, 1991; Toro et al., 1998; Vergara et al., 1998). The BK channel is a homotetramer of its pore-forming α-subunit, which is coded by the gene *Slo1* (KNCMA1). This protein contains seven putative transmembrane segments (S0–S6) where the primary sequence of S1–S6 is homologous to the corresponding domains in K_V channels (Shen et al., 1994; Meera et al., 1997). The channel is gated both by membrane depolarization and by increased intracellular Ca^{2+} concentration. Thorough studies of BK channel gating suggest that calcium and voltage act as allosteric modulators (Cox et al., 1997; Cox and Aldrich, 2000; Horrigan and Aldrich, 2002).

In some mammal tissues, BK channel α subunits are coexpressed with modulatory β subunits, four of which have been cloned (Knaus et al., 1994b; Jiang et al., 1999; Wallner et al., 1999; Xia et al., 1999; Behrens et al., 2000; Brenner et al., 2000; Meera et al., 2000; Uebele et al., 2000; for review see Orio et al., 2002). Purification and cloning of the β1-subunit unveiled the presence of a protein containing two putative transmembrane regions joined together by a large extracellular loop (Knaus et al., 1994a,b). β1 increases the apparent Ca^{2+} sensitivity of the channel, slows down the macroscopic activation and deactivation kinetics, and decreases the voltage sensitivity (McManus et al., 1995; Wallner et al., 1995; Dworetzky et al., 1996; Meera et al., 1996; Cox and Aldrich, 2000; Nimigean and Magleby, 2000; Bao and Cox, 2005; Orio and Latorre, 2005). The presence of the β1-subunit is also a requirement for the binding of channel activators (McManus et al., 1995; Valverde et al., 1999; Dick et al., 2001). The S0 domain and the extracellular NH_2 terminus of the α-subunit are crucial for the adequate functional coupling between α- and

P. Orio and Y. Torres contributed equally to this work.
Correspondence to Ramon Latorre: rlatorre@cecs.cl
P. Orio's present address is the Instituto de Neurociencias de Alicante, Universidad Miguel Hernandez-CSIC, 03550 Sant Joan d'Alacant, Spain.
P. Rojas's present address is the Department of Anatomy and Neurobiology, Washington University School of Medicine, St. Louis, MO 63110

β1-subunit (Wallner et al., 1996). The β2-subunit has an N-type or fast inactivation motif in its NH_2 terminus, causing BK currents to inactivate when this subunit is present (Wallner et al., 1999; Xia et al., 1999). This motif can be removed (β2IR-subunit) and the activation properties of the channel can be studied in the presence of β2IR without the contamination of the inactivation process. Like the β1-subunit, β2IR also increases the apparent Ca^{2+} sensitivity of the BK channels and slows down its macroscopic kinetics (Wallner et al., 1999; Xia et al., 1999). But unlike the β1-subunit, β2IR does not modify the voltage dependence and confers low affinity to CTX compared with that exhibited by the α-subunit (Xia et al., 1999; Orio and Latorre, 2005).

Although the region in the α-subunit responsible for β1-subunit regulation has been mapped to the S0 membrane-spanning and NH_2-terminal regions, very little is known about the structural determinants contained in the β subunits that determine the functional coupling between α and β subunits. We showed in detail that β1 and β2IR subunits conferred different gating properties to the BK channel (Orio and Latorre, 2005). In particular, they impart to BK channels different calcium sensitivities, voltage dependences, and macroscopic gating kinetics. Here we use these differences to map the regions in the β subunits responsible for β-subunit regulation by constructing chimeras between β1 and β2IR subunits. Our results show that intracellular NH_2 and COOH termini are responsible for most of the modulatory effects on channel activity, with some participation of the transmembrane regions. The extracellular regions have no participation in the differences between β1 and β2IR subunits and may play a structural function related to other effects of the β subunits on the channel.

MATERIALS AND METHODS

DNA Clones

cDNAs coding for BK channel α-subunit (KCNMA1) from myometrium (GenBank/EMBL/DDBJ accession no. U11058), human β1 and β2 subunits (KCNMB1 and KCNMB2, GenBank/EMBL/DDBJ accession no. U25138 and AF099137), and β2-subunit without inactivation domain (β2IR) (Wallner et al., 1999) were used. The boundaries of the transmembrane domains of β1 and β2IR subunits were defined according to Wallner et al. (1999). Chimeric β subunits were made with the overlapping extension method (Horton et al., 1990) and confirmed by DNA sequencing.

Channel Expression

mMESSAGE mMACHINE (Ambion) in vitro transcription kit was used to obtain mRNAs. Channels were expressed in *Xenopus* oocytes using standard techniques (Stühmer and Parekh, 1995). α-Subunit cRNA (0.75 to 2 ng) or a mixture of α-subunit (0.5–1.5 ng) and β-subunit (2–3 ng) cRNAs were injected per oocyte. The approximate molar ratio was at least 6:1 (β:α), ensuring saturation of β-subunit.

Electrophysiological Recordings and Solutions

Currents were recorded 1–5 d after cRNA injection using the inside-out configuration of the patch-clamp technique. All recordings were performed at room temperature (20–22°C). Intracellular (bath) and extracellular (pipette) solutions contained (in mM) 110 KOH, 10 HEPES, and 2 KCl and were adjusted to pH 7.4 with methanosulfonic acid. Depending on the desired free calcium concentration, 1.8–3.5 mM $CaCl_2$ and 5 mM EGTA (5–200 nM), HEDTA (0.6–12 μM), or NTA (20–150 μM) was added. Free calcium concentrations were calculated using the WinMaxChelator Software (http://www.stanford.edu/~cpatton/maxc.html) and checked with a calcium electrode (World Precision Instruments). The solution designated as "5 nM" is an upper estimation based on contaminating calcium. Depending on the magnitude of currents, and in order to minimize voltage drops due to series resistance, some experiments were done with solutions containing 36 mM KOH and 74 mM NMDG. The pipette solution contained 100 nM or lower free calcium.

Pipettes were pulled in a horizontal pipette puller (Sutter Instruments) from Corning 7740 (Pyrex) or Custom 8250 (Warner Instruments) borosilicate capillary glass. Pipette resistance was 0.8–2 MΩ in 110 mM K^+, and series resistance error was always <10 mV.

Data were acquired with an Axopatch 200B (Axon Instruments) or an EPC-7 (List Medical) amplifier, filtered with an 8-pole Bessel filter (Frequency Devices) at 1/5 of the acquisition rate, and sampled with a 16-bit A/D converter (NI-6036, National Instruments). Typical acquisition rates ranged from 66.6 to 100 kHz (α-subunit alone) or from 16.6 to 40 kHz (α + β subunits). Homemade acquisition software was developed in the LabView programming environment (National Instruments). Primary data analysis was performed with Analysis (provided by F. Bezanilla, University of California Los Angeles, CA) and Clampfit 9 (Axon Instruments) software.

Steady-state Activation Analysis

The Solver function of Microsoft Excel was used to fit a Boltzmann function of the form

$$I = \frac{I_{\max}}{1 + \exp\left(-\frac{zF(V - V_{0.5})}{RT}\right)} \quad (1)$$

to instantaneous tail currents, where I_{max} is the maximum obtained tail current, z is the voltage dependency of activation, $V_{0.5}$ is the half-activation voltage, T is the absolute temperature (typically 295K), F is the Faraday's constant, and R is the universal gas constant. When $[Ca^{2+}]$ was <500 nM, only low conductances were achieved and the estimation of I_{max} became unreliable. In those cases, I_{max} was fixed using the value obtained with higher calcium concentrations in the same patch. All the analysis that follows was performed using I/I_{max} values.

Statistical Analysis

The τ_{act}/V curves were compared by a two-way ANOVA test, thus assessing the statistical significance of the datasets as a whole. The $V_{0.5}/[Ca^{2+}]$ curves could not be compared by a two way ANOVA test because not all the chimeras were studied at the same calcium concentrations. Instead, the statistical difference between two datasets was performed by testing whether they can be fit by two (independent fit) or a single (global fit) dose–response curve. Comparison between independent and global fits was done by an extra sum-of-squares F test, using the formula

$$F = \frac{\left(SS_{glb} - SS_{ind}\right)/\left(DF_{glb} - DF_{ind}\right)}{SS_{ind}/DF_{ind}},$$

where *SS* and *DF* are the sum-of-squares and the degrees of freedom of the fit, respectively. *glb* and *ind* denote the global and the independent fit, respectively. The same procedure was used to test the difference of the exponential factors for the τ_{deact} values in the −50 to 60 mV range. The z values showed the greatest variability

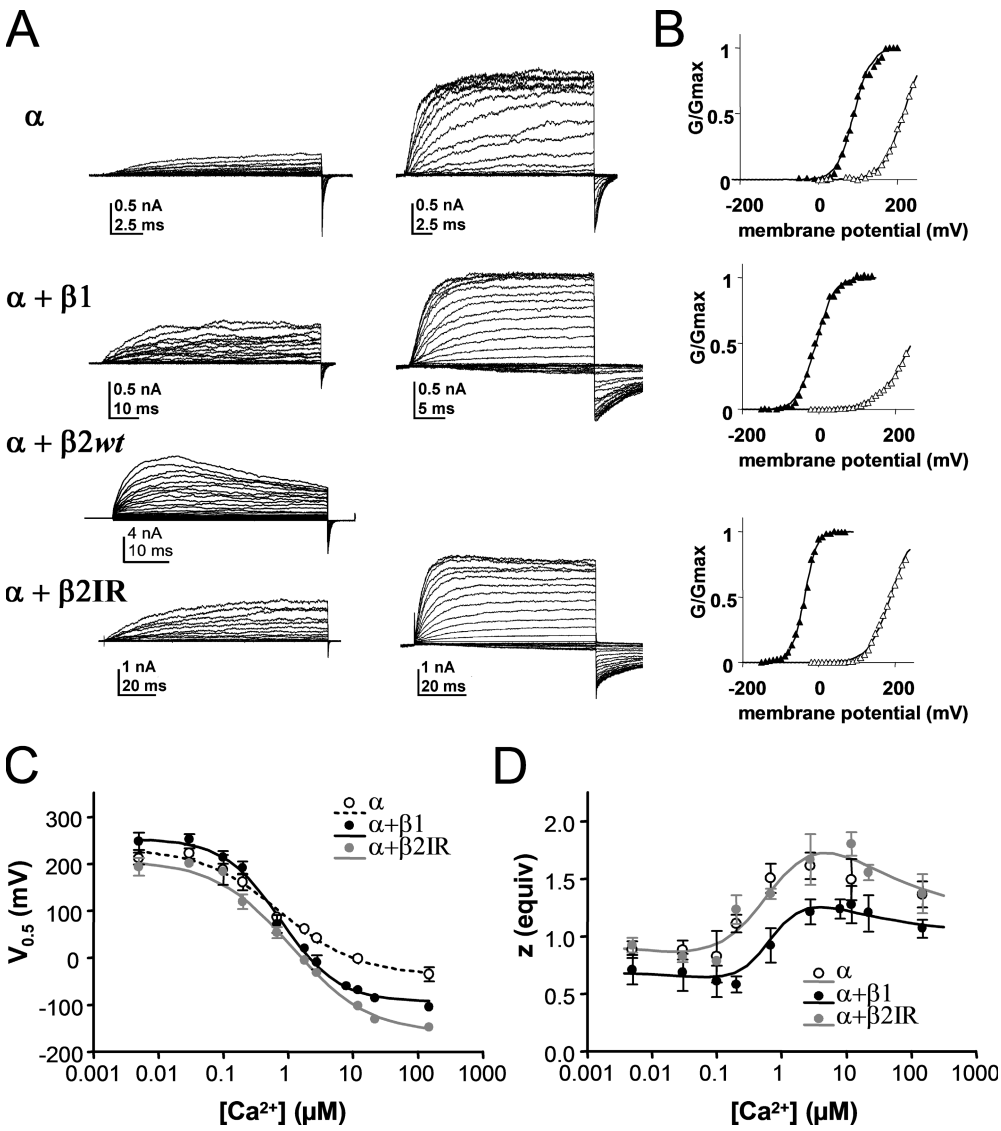

Figure 1. Effects of β1 and β2IR subunits on BK channel steady-state activation parameters. (A) Macroscopic currents recorded in the inside-out configuration at 5 nM (left) and 3 μM (right) intracellular calcium. The voltage protocol for 5 nM was: holding potential (HP), 0 mV; prepulse (PP), −80 mV; test pulse (TP), −10 to 250 mV in 10-mV steps; tail, −60 mV. The voltage protocol for 3 μM was: HP, 0 mV; PP, −150 mV; TP, −150 to 140 in 10-mV steps; tail, −60 mV. (B) Normalized G/V curves at 3 μM (closed symbols) and 5 nM Ca^{2+} (open symbols) for the α, α + β1 and α + β2IR current traces shown in A. Lines are the best fit of a Boltzmann distribution (Eq. 1). Fit parameters are as follows. α, $V_{0.5}$ = 215 mV, z = 0.95 (5 nM); $V_{0.5}$ = 91 mV, z = 1.19 (3 μM). α + β1, $V_{0.5}$ = 243 mV, z = 0.61 (5 nM); $V_{0.5}$ = −7 mV, z = 1.11 (3 μM). α + β2IR, $V_{0.5}$ = 189 mV, z = 0.91 (5 nM); $V_{0.5}$ = −37 mV, z = 1.58 (3 μM). (C) Average of the obtained $V_{0.5}$ values plotted against calcium concentration. A best fit sigmoid concentration–effect curve was added as reference for visual comparison in the following figures. (D) Average of the obtained z values plotted against calcium concentration. A best fit dual effect sigmoid curve was added as reference for visual comparison in the following figures. Error bars are SD, n = 7–8. When SD bars are not visible, they are smaller than symbol size.

of all the parameters studied, and the statistical comparisons were not reliable. All the analyses were done with the GraphPad Prism software (GraphPad Software Inc.).

RESULTS

Differential Modulation of the BK Channel by its β1 and β2 Subunits

In a previous report (Orio and Latorre, 2005) we showed clear differences in the way that the β1 and β2 subunits modulate BK channel's properties, suggesting a different mechanism of action. The differences in the modulation of steady-state activation of the channel are summarized in Fig. 1. As the β2-subunit induces a fast or N-type inactivation of the current (Fig. 1 A, β2*wt*), in the previous as well as in this work we studied a truncated β2-subunit (Δ2-19β2, β2IR) that lacks the inactivation peptide. In the presence of the β2IR-subunit, BK currents are sustained (Fig. 1 A, α+β2IR) and therefore the effects of this subunit in the activation parameters of the BK channel are best studied.

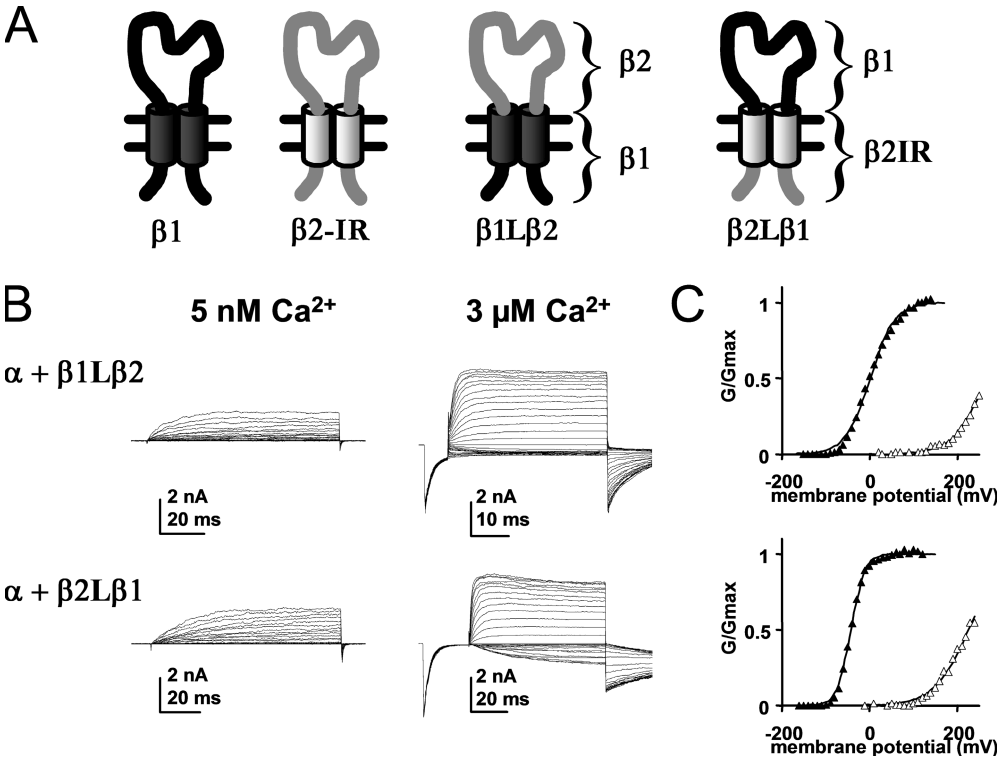

Figure 2. Effects of β1Lβ2 and β2Lβ1 subunits on BK channel steady-state activation parameters. (A) Schematic description of the β1Lβ2 and β2Lβ1 chimeras. (B) Macroscopic currents recorded in the inside-out configuration at 5 nM (left) and 3.3 μM (right) intracellular calcium, for α + β1Lβ2 (top) and α + β2Lβ1 (bottom) channels. The voltage protocols are as described in legend of Fig. 1. (C) Normalized G/V curves at 3.3 μM (closed symbols) and 5 nM Ca^{2+} (open symbols) for the current traces shown in B. Lines are the best fit of a Boltzmann distribution (Eq. 1). Fit parameters are as follows. α + β1Lβ2, $V_{0.5}$ = 267 mV, z = 0.7 (5 nM); $V_{0.5}$ = 2 mV, z = 0.92 (3.3 μM). α + β2Lβ1, $V_{0.5}$ = 226 mV, z = 0.65 (5 nM); $V_{0.5}$ = −42 mV, z = 1.7 (3.3 μM).

A convenient way to represent the voltage and calcium sensitivity of the BK channel is by fitting the G/V curve to a Boltzmann distribution (Eq. 1; Fig. 1 B). The half-activation voltage ($V_{0.5}$) reports the position of the curve along the voltage axis while the z value reports the voltage sensitivity of the channel. Increasing the calcium concentration lowers the half-activation voltage (Fig. 1 C) and in the presence of both the β1 and β2IR subunits the effect of calcium is enhanced, as the $V_{0.5}$ values for α+β1 and α+β2IR are lower than for α at $[Ca^{2+}] \geq 1$ μM. However, the half potential shift to more hyperpolarized voltages is more pronounced in α + β2IR channels. At $[Ca^{2+}] \leq 100$ nM, α+β1 channels have higher values than either α or α+β2IR channels while α+β2IR is not different from α. Finally, the β1-subunit produces a reduction in the BK voltage dependence, not observed when channels are formed by α + β2IR subunits (Fig. 1 D).

In the case of the kinetic parameters, both β subunits slow down the activation kinetics. However, α + β2IR channels show a slower activation and the voltage dependence of the deactivation kinetics is modified by the presence of the β1- but not the β2-subunit (Orio and Latorre, 2005; see also Fig. 4, C and D).

The External Loop of β Subunits Is Not Involved in Differential Coupling

The rationale of the experiments that follow is based upon the electrophysiological differences shown by channels formed by α + β1 and α + β2IR subunits. We, therefore, predicted that regions essential for β-subunit modulation of the BK channel may be identified by exchanging regions between β1 and β2 subunits. The first set of chimeras tested was one in which the external loops were exchanged: β2 containing the loop of β1 (β2Lβ1) and β1 containing the loop of β2 (β1Lβ2) (Fig. 2 A). Fig. 2 B shows that coexpression of these chimeras with the α-subunit produces robust currents in excised patches of oocyte membrane. In particular, it is apparent from the current records that both chimeras are able to slow down the activation and deactivation kinetics with respect to currents generated by α-subunit alone (see also Fig. 4). Fig. 2 C shows that the conductance is voltage and Ca^{2+} dependent. A more detailed inspection indicates that the G/V curves for the β2Lβ1 chimera are steeper and that at 3 μM Ca^{2+} it is shifted ∼40 mV to the left compared with the β1Lβ2 chimera. To quantify the effects of each chimera and to have an adequate comparison of their characteristics with those

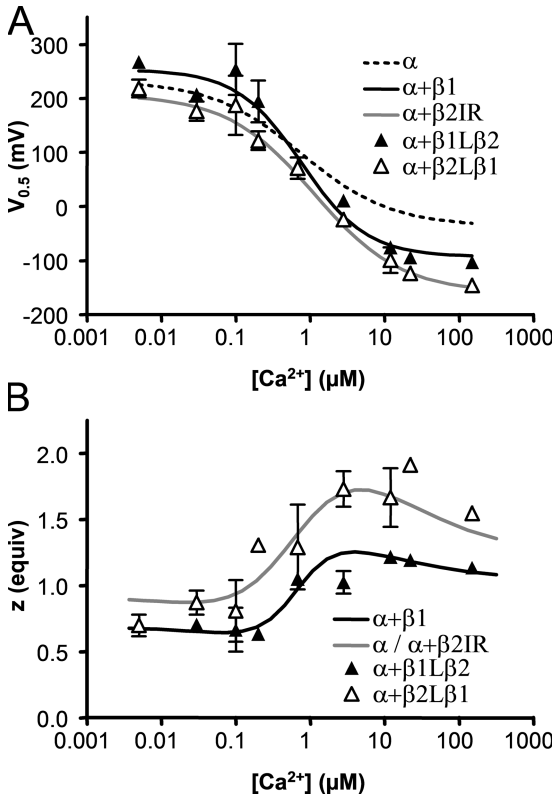

Figure 3. Steady-state activation parameters for α + β1Lβ2 and α + β2Lβ1 channels. (A) Average of the obtained $V_{0.5}$ values plotted against calcium concentration. For α, α + β1, and α + β2IR only the best fit sigmoid concentration–effect curve (see Fig. 1 C) is depicted. (B) Average of the obtained z values plotted against calcium concentration. For α, α + β1, and α + β2IR only the best fit curve (see Fig. 1 D) is depicted. Error bars are SD, n = 5–6. When SD bars are not visible, they are smaller than symbol size.

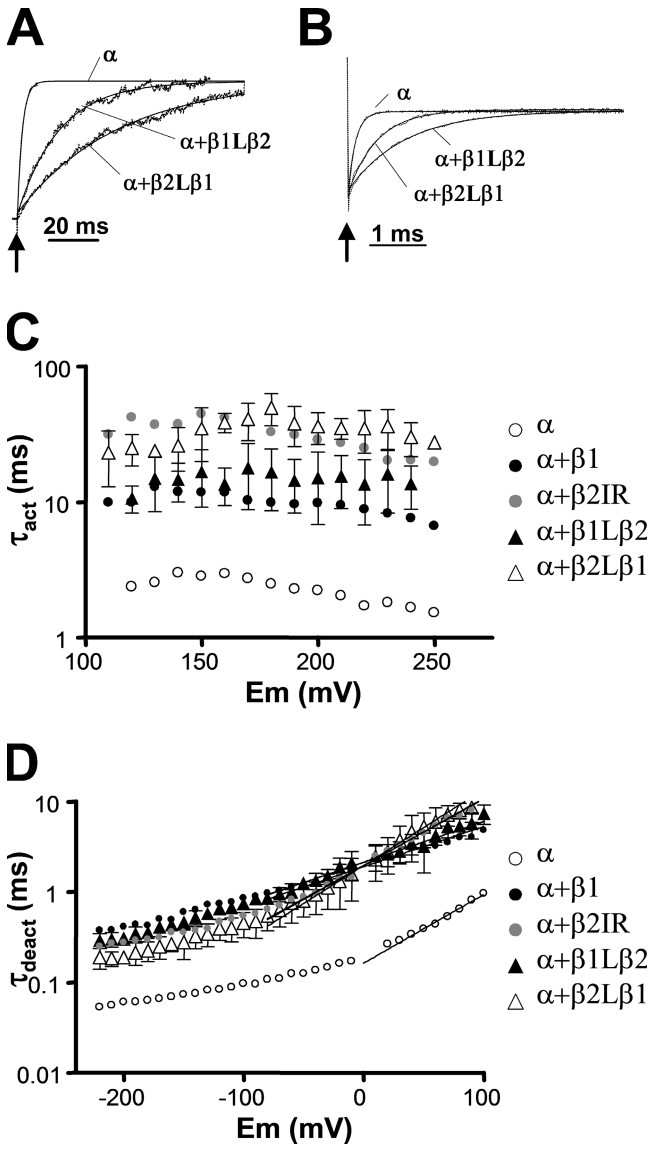

Figure 4. Effect of the β1Lβ2 and β2Lβ1 subunits on BK channel macroscopic kinetics in the absence of calcium. (A) Current traces evoked by a 200 mV pulse after a −80 mV prepulse. Over the traces, the best fit to an exponential raise is shown. Current magnitude of each trace was normalized by the steady-state current predicted by the fit. For α, the fit was extrapolated to show that the traces are effectively normalized to the same maximum. (B) Tail current traces evoked by a −60 mV pulse after opening the channels with a +200 mV activation pulse. Current magnitude of each trace was normalized by the peak of the tail current. Over the traces, the best fit to an exponential decay is shown. (C) Activation time constant (τ_{act}) plotted against activation voltage. Symbols represent mean ± SD. n = 7–10. (D) Deactivation time constant (τ_{deact}) plotted against voltage. Symbols represent mean ± SD. n = 3–5. In the case of α, α + β1, and α + β2IR, only the mean is shown. Lines represent the best fit of a single exponential function to the data between −50 and +60 mV extrapolated from −80 to +100 mV.

of the parent β subunits we performed experiments over a wide range of Ca^{2+} concentrations. Fig. 3 (A and B) summarizes the results obtained from the fitting of the G/V curves to Eq. 1. Fig. 3 A shows a plot of $V_{0.5}$ against [Ca^{2+}] for β1Lβ2 (black triangles) and β2Lβ1 (open triangles). Fig. 3 B shows the z values against [Ca^{2+}] for β1Lβ2 (black triangles) and β2Lβ1 (open triangles). For visual comparison purposes, the data for α, α + β1, and α + β2IR channels are shown only as the best fit curves (see figure legends for details). The results demonstrate that the behavior of channels formed by α + β1Lβ2 resembles that of channels produced by the coexpression of α + β1 (P = 0.6 and 0.002 compared with α + β1 and α + β2IR, respectively, in an extra sum-of-squares F test; see MATERIALS AND METHODS) and that the activity of channels formed by α + β2Lβ1 is similar to channels formed by α + β2IR (P = 0.002 and 0.72 compared with α + β1 and α + β2IR, respectively). This result suggests that the loop region is not responsible for the functional differences between β1 and β2 subunits.

As mentioned before, both β1 and β2IR subunits slow down the activation process of the channel but the time course of the current induced by α + β2IR channels is slower than that promoted by α + β1 channels (Orio and Latorre, 2005). Fig. 4 A shows representative

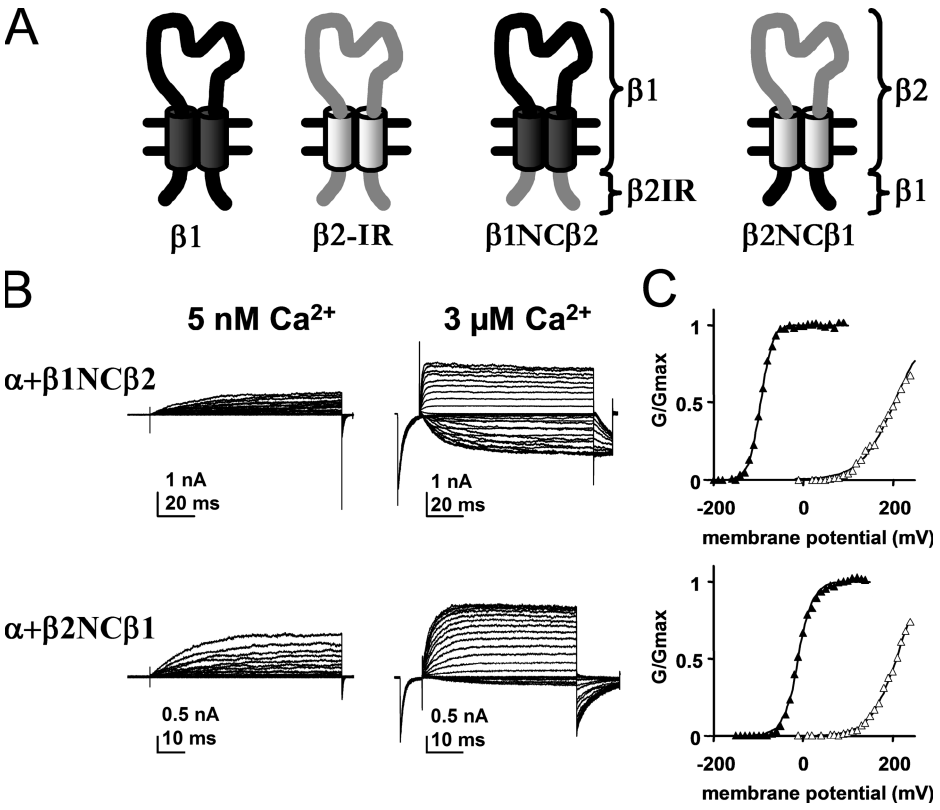

Figure 5. Effects of β1NCβ2 and β2NCβ1 subunits on BK channel steady-state activation parameters. (A) Schematic description of the β1NCβ2 and β2NCβ1 chimeras. (B) Macroscopic currents recorded in the inside-out configuration at 5 nM (left) and 3.3 μM (right) intracellular calcium, for α + β1NCβ2 (top) and α + β2NCβ1 (bottom) channels. The voltage protocols are as described in legend of Fig. 1. (C) Normalized G/V curves at 3.3 μM (closed symbols) and 5 nM Ca^{2+} (open symbols) for the current traces shown in B. Lines are the best fit of a Boltzmann distribution (Eq. 1). Fit parameters are as follows. α + β1NCβ2, $V_{0.5}$ = 204 mV, z = 0.7 (5 nM); $V_{0.5}$ = −95 mV, z = 2.0 (3.3 μM). α + β2NCβ1, $V_{0.5}$ = 208 mV, z = 0.9 (5 nM); $V_{0.5}$ = −10 mV, z = 1.5 (3.3 μM).

current traces for channel activation at 200 mV after a −80 hyperpolarizing pulse in the virtual absence of calcium (5 nM). The time course followed by the currents induced by α + β2Lβ1 channels is slower than that of α + β1Lβ2 channels. Fig. 4 C plots the time constant of an exponential fit of the current time course as a function of the activation voltage. The tendency (α + β2Lβ1 slower than α + β1Lβ2 slower than α) is maintained at all the activation voltages explored, resembling the behavior of the β1 and β2IR subunits. As in the $V_{0.5}/[Ca^{2+}]$ and $z/[Ca^{2+}]$ plots, the data obtained for α + β1Lβ2 channels superimposes to that obtained for α + β1 channels (P = 0.13 and $P < 0.0001$ when compared with α + β1 and α + β2IR, respectively, in a two-way ANOVA test), and the data obtained for α + β2Lβ1 channels is not different from that obtained for α + β2 channels ($P < 0.0001$ and P = 0.94 when compared with α + β1 and α + β2IR, respectively).

The deactivation process at −60 mV after a 200-mV activation pulse is also slower when the channel is coexpressed with the chimeric subunits β1Lβ2 and β2Lβ1 (Fig. 4 B). Moreover α + β1Lβ2 is slower than α + β2Lβ1, confirming that β1Lβ2 behaves like β1 while β2Lβ1 is like β2IR. However, the deactivation kinetics must be studied in a wide voltage range because the β1-subunit also affects the voltage dependence of the deactivation process. Fig. 4 D plots the deactivation time constant (τ_{deact}) in the −220 to +100 mV voltage range. The semilogarithmic τ_{deact}/V plot shows two apparent slopes for all α, α + β1, and α + β2IR channels. While the first slope (limiting slope for the voltage dependence of channel deactivation) is not affected by the type of β-subunit, the second slope (z = 0.44 electronic equivalents for the α-subunit alone) is severely affected by the β1 (z = 0.25) but not the β2IR (z = 0.44) subunit. This is due to the reduction of the voltage sensor–associated voltage dependence of the BK channel that occurs in the presence of the β1-subunit (Orio and Latorre, 2005; but see Bao and Cox, 2005). The chimeric β1Lβ2-subunit modifies the voltage dependence of the deactivation process of the channel in the same way as the β1-subunit, with a z value of 0.28 (P = 0.8 and $P < 0.0001$ compared with α + β1 and α + β2IR, respectively, in an extra sum-of- squares F test). The β2Lβ1-subunit shows a voltage sensor–related slope a little higher than that observed for α + β2IR channels (z = 0.48, $P < 0.0001$ and P = 0.003 compared with α + β1 and α + β2IR, respectively).

These results strongly suggest that the differential effects of the β subunits on the BK channel properties are related to the transmembrane and/or the intracellular domains of these regulatory subunits but not to the extracellular domain.

Functional Coupling Is Mainly Determined by Intracellular Domains

To circumscribe the structure(s) in the β subunits determining the differential coupling with the α-subunit,

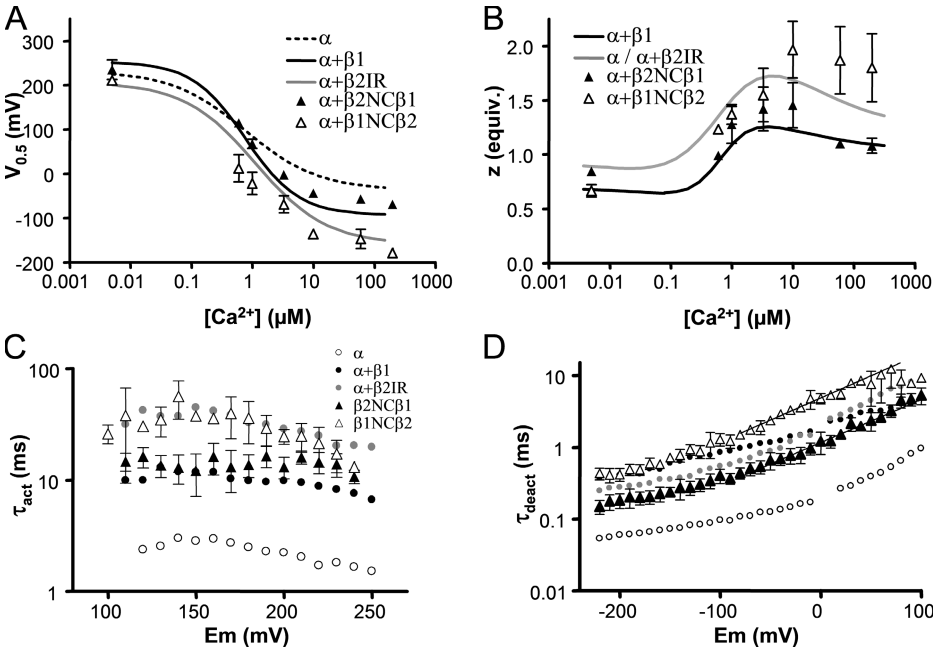

Figure 6. Activation parameters for α + β1NCβ2 and α + β2NCβ1 channels. (A) Average of the obtained $V_{0.5}$ values plotted against calcium concentration. For α, α + β1, and α + β2IR, only the best fit sigmoid concentration–effect curve (see Fig. 1 C) is depicted. (B) Average of the obtained z values plotted against calcium concentration. For α, α + β1, and α + β2IR only the best fit curve (see Fig. 1 D) is depicted. Error bars are SD, $n = 4$–7. When SD bars are not visible, they are smaller than symbol size. (C) Activation time constant (τ_{act}) at 5 nM intracellular [Ca^{2+}] plotted against activation voltage. Symbols represent mean ± SD. $n = 3$–5. (D) Deactivation time constant (τ_{deact}) at 5 nM intracellular [Ca^{2+}] plotted against voltage. Symbols represent mean ± SD. $n = 3$–7. In the case of α, α + β1, and α + β2IR, only the mean is shown. Lines are defined as in Fig. 4.

we exchanged the NH_2 and COOH terminus between β1 and β2IR. The two chimeras generated in this way were denominated β1NCβ2 (β1 with NH_2 and COOH termini of β2) and β2NCβ1 (β2 with NH_2 and COOH termini of β1) (Fig. 5 A). Fig. 5 B shows that the coexpression of both chimeras with the BK channel produces robust, calcium- and voltage-dependent currents. From the G/V plots (Fig. 5 C), it is evident that in the presence of the β1NCβ2 chimera, the channel has higher calcium sensitivity than in the presence of β2NCβ1 (the curve for 3 μM is more displaced to the left). Also, α + β1NCβ2 channels have a higher voltage dependency. The analysis of the calcium and voltage dependence (Fig. 6, A and B) in the presence of these chimeras shows that the β2NCβ1 chimera (filled triangles) imparts to the BK channel similar properties than those obtained when the α-subunit is coexpressed with the β1-subunit (black solid line), both in terms of the $V_{0.5}/[Ca^{2+}]$ ($P = 0.03$ and $P < 0.0001$ compared with α + β1 and α + β2IR, respectively) as well as the $z/[Ca^{2+}]$ relationships. The β1NCβ2 chimera (empty triangles) on its hand resembles the behavior of the β2IR (gray solid lines) subunit, though the $V_{0.5}$ values are displaced 40–50 mV toward more negative voltages ($P < 0.0001$ and $P = 0.003$ compared with α + β1 and α + β2IR, respectively).

β1NCβ2 and β2NCβ1 chimeras also show an effect on channel kinetics, slowing down both the activation and deactivation processes. Fig. 6 C plots the time constant of the macroscopic activation kinetics (τ_{act}) at several voltages and in the absence of calcium. β1NCβ2 resembles the behavior of the β2IR-subunit ($P < 0.0001$ and $P = 0.08$, respectively) and though the β2NCβ1 is statistically different from both ($P = 0.0002$ and $P < 0.0001$, respectively), it is closer to the β1-subunit. This suggests that the intracellular portions of the β subunits are responsible for the modulation of the activation kinetics.

In the case of the macroscopic deactivation kinetics (Fig. 6 D), none of the chimeras behaved exactly as either the β1- or the β2IR-subunit. The voltage dependence of the deactivation kinetics turned out to be different to both parent β subunits ($z = 0.35 \pm 0.02$ for α + β2NCβ1 and 0.36 ± 0.02 for α + β1NCβ2 channels; $P \leq 0.01$ for all comparisons with α + β1 and α + β2IR), suggesting a partial effect on the voltage sensor–associated voltage dependence. α + β1NCβ2 channels have τ_{deact} limiting values (at the most negative potentials) close to α + β1 channels ($P = 0.03$), indicating that the kinetic rate for channel deactivation when all voltage sensors are in the resting position is affected by this chimera in the same way as in the presence of the β1-subunit.

In summary, the study of the "NC" chimeras suggests that the intracellular regions of the β1 and β2IR subunits determine the modulation of a great part of the properties studied here, with the exception of the

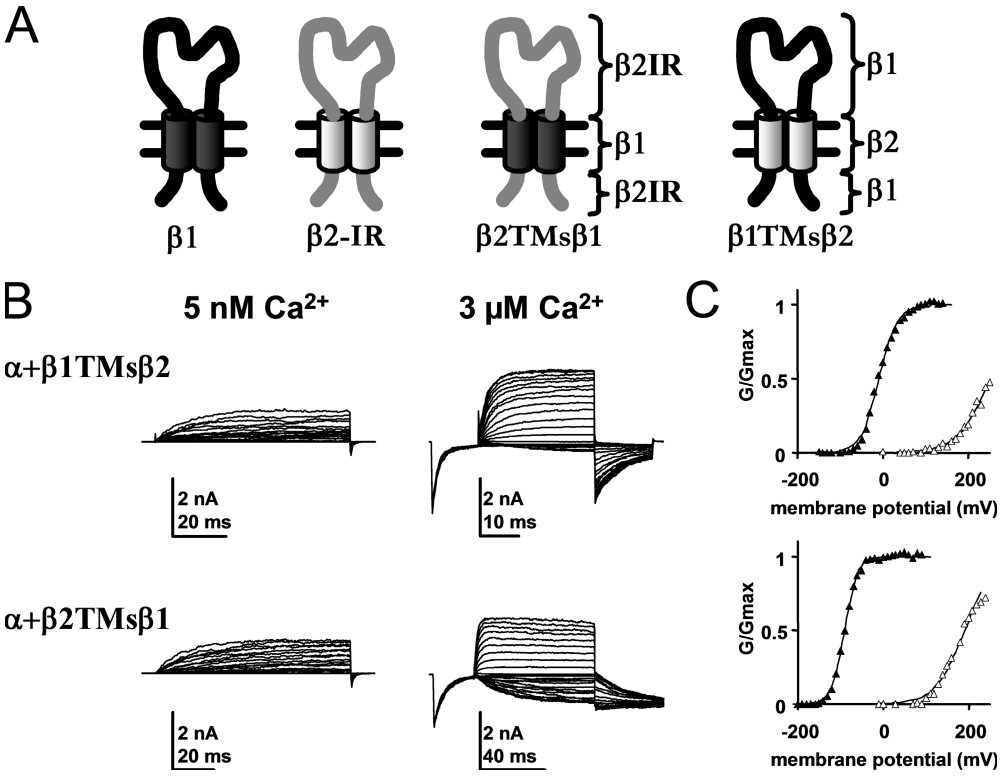

Figure 7. Effects of β1TMsβ2 and β2TMsβ1 subunits on BK channel steady-state activation parameters. (A) Schematic description of the β1TMsβ2 and β2TMsβ1 chimeras. (B) Macroscopic currents recorded in the inside-out configuration at 5 nM (left) and 3.3 μM (right) intracellular calcium, for α + β1TMsβ2 (top) and α + β2TMsβ1 (bottom) channels. The voltage protocols are as described in legend of Fig. 1. (C) Normalized G/V curves at 3.3 μM (closed symbols) and 5 nM Ca^{2+} (open symbols) for the current traces shown in B. Lines are the best fit of a Boltzmann distribution (Eq. 1). Fit parameters are as follows. α + β1TMsβ2, $V_{0.5}$ = 251 mV, z = 0.7 (5 nM); $V_{0.5}$ = −9 mV, z = 1.2 (3.3 μM). α + β2TMsβ1, $V_{0.5}$ = 191 mV, z = 0.7 (5 nM); $V_{0.5}$ = −90 mV, z = 1.7 (3.3 μM).

changes induced in the deactivation kinetics and its voltage dependence. Essentially the same conclusion can be obtained from the analysis of the β1TMβ2 and β2TMβ1 chimeras, in which the transmembrane domains were exchanged between β1 and β2IR (Figs. 7 and 8). β2TMβ1 chimera, which contains the same intracellular domains as β2 and β1NCβ2 subunits, behaves very much like the β1NCβ2 subunits. On the other hand, the β2TMβ1 chimera, which contains the same intracellular domains as the β1 and β2NCβ1 subunits, behaves as the β2NCβ1 chimera. This can be seen from another point of view: the β1NCβ2 and β2TMβ1 chimeras modulate BK channel properties in a very similar way and they share the transmembrane and intracellular domains with a completely different extracellular loop. The same is true for the β2NCβ1 and β1TMβ2 chimeras. This is in complete agreement with the results of the β1Lβ2 and β2Lβ1 chimeras, as the extracellular loop does not determine the differential behavior of the β subunits.

The NH_2 Terminus Is Crucial for Defining the Behavior of either β-subunit

To define further the functional coupling structures, we next created chimeras in which the NH_2 terminus (β1Nβ2, β2Nβ1) or the COOH terminus (β1Cβ2, β2Cβ1) between β1 and β2IR was exchanged (Fig. 9 A and Fig. 10 A).

When the NH_2 terminus of β2IR is transplanted into the β1-subunit, the resulting chimera (β1Nβ2) confers to the BK channel many of the properties of the β2-subunit: the α + β1Nβ2 channels are very similar to α + β2IR in terms of the $V_{0.5}$ (Fig. 9 B, P = 0.02 and P = 0.1 compared with α + β1 and α + β2IR, respectively), z (Fig. 9 C), and τ_{act} (Fig. 9 D, $P < 0.0001$ and $P = 0.6$, respectively) values. The only reminiscences of the β1-subunit are found in the τ_{deact}/V plot, where the voltage sensor–associated voltage dependence (z = 0.28, P = 0.02 and $P < 0.0001$, respectively) and the limiting τ_{deact} value are similar to α + β1. Something similar occurs with the opposite chimera, β2Nβ1, with some minor differences. α + β2Nβ1 channels behave like α + β1 in terms of the z (Fig. 9 C) and τ_{act} (Fig. 9 D, P = 0.5 and $P < 0.0001$, respectively) values; however, the $V_{0.5}$ values fall between the curves for α alone and α + β1 channels (Fig. 9 B; P = 0.001 when compared with α + β1 and 0.07 when compared with α). The latter may be an indication of a disruption of the effect of the β subunits on the apparent calcium sensitivity. Regarding the

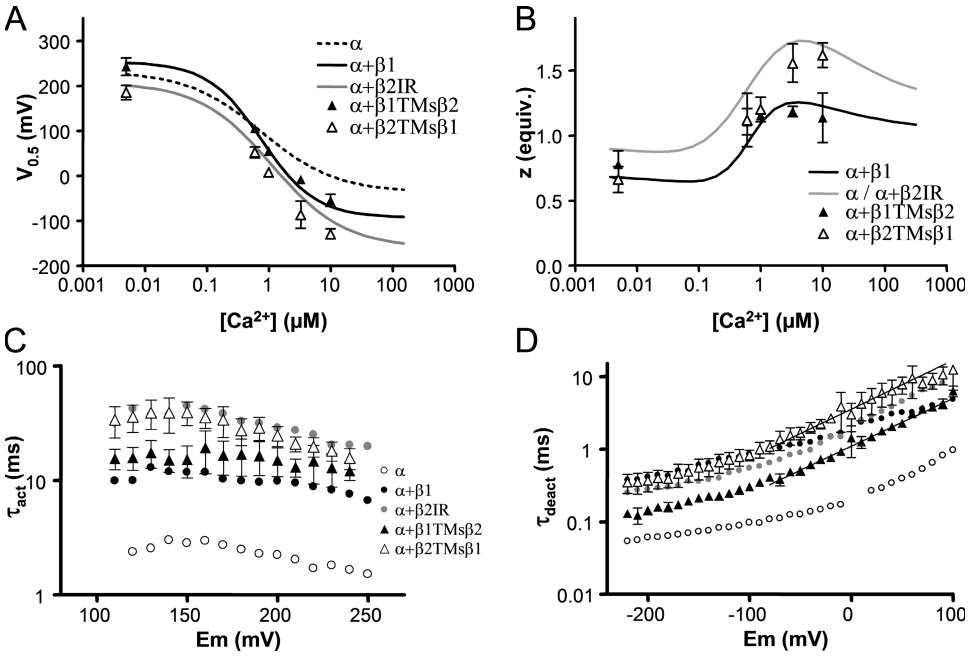

Figure 8. Activation parameters for α + β1TMsβ2 and α + β2TMsβ1 channels. (A) Average of the obtained $V_{0.5}$ values plotted against calcium concentration. For α, α + β1, and α + β2IR, only the best fit sigmoid concentration–effect curve (see Fig. 1 C) is depicted. (B) Average of the obtained z values plotted against calcium concentration. For α, α + β1, and α + β2IR, only the best fit curve (see Fig. 1 D) is depicted. Error bars are SD, n = 5–6. Missing error bars are smaller than symbol size. (C) Activation time constant (τ_{act}) at 5 nM intracellular [Ca^{2+}] plotted against activation voltage. Symbols represent mean ± SD. n = 6–8. (D) Deactivation time constant (τ_{deact}) at 5 nM intracellular [Ca^{2+}] plotted against voltage. Symbols represent mean ± SD. n = 4–5. In the case of α, α + β1, and α + β2IR, only the mean is shown. Lines are defined as in Fig. 4. The exponent factors expressed as electronic charges (z = slope × RT/F) are α + β1TMsβ2, 0.39 ± 0.01; α + β2TMsβ1, 0.39 ± 0.02.

deactivation kinetics, the behavior is intermediate between α and α + β2IR channels, with a lower limiting τ_{deact} than α + β2IR and a slope for the −50 to +50 voltage range of 0.34 ($P < 0.01$ when compared with both α + β1 and α + β2IR).

When the COOH termini of the β1 and β2IR subunits are transplanted between each other, the resulting chimeras have almost all the properties of the parent β-subunit. The α + β1Cβ2 channels have $V_{0.5}$ values ($P = 0.05$ and $P < 0.0001$), z values, τ_{act} values ($P = 0.3$ and $P < 0.0001$), and τ_{deact} voltage dependence of α + β1 (Fig. 10, B–E); only the limiting τ_{deact} resembles that of α + β2IR (Fig. 10 E; $P = 0.2$). α + β2Cβ1 channels, on the other hand, behave like α + β2IR in terms of the z (Fig. 10 C), τ_{act} (Fig. 10 D; $P < 0.0001$ and $P = 0.07$, respectively), and τ_{deact} values (Fig. 10 E; $P < 0.0001$ and $P = 0.3$, respectively, for the −50 to 50 mV slope). Interestingly, the $V_{0.5}$ values are like α + β1 ($P = 0.7$ and $P = 0.0001$, respectively), suggesting again a partial disruption of the normal effect of the β2IR-subunit on the apparent calcium sensitivity.

In summary, a gross analysis of the results with the "N" and "C" chimeras indicates that most of the differences between β1 and β2IR subunits reside in the corresponding NH_2 terminus, and that for some of the effects (changes in τ_{deact}, for example) both intracellular domains are required.

DISCUSSION

Structural Determinants in α–β Subunit Coupling

The extracellular NH_2 terminus of the α-subunit together with the first transmembrane domain S0 have been proposed to contribute to the functional interaction between β and α subunits (Wallner et al., 1996). This conclusion was put forward based on the results obtained using different chimeras between *hSlo* and the *Drosophila* homologue of *hSlo*, *dSlo*, that does not functionally couple to the β1-subunit. A chimera containing only the extracellular NH_2 terminus together with the first transmembrane domain S0 of *hSlo* is able to successfully couple with the β1-subunit. Here we attempt to draw similar conclusions from the side of the β1 and β2 subunits, characterizing a set of chimerical β subunits. A general view of our results shows that the intracellular regions of β1 and β2 are responsible for most of the differences between the modulatory effects that each of them confer to the activity of BK channel.

The β1 and β2 subunits are the most closely related within the BK channel's β-subunit family, with a 43% overall sequence identity and a 39% identity in the loop region. Leaving aside the inactivation promoted by the β2-subunit, they have qualitatively similar effects on BK channel properties. Our conclusions, therefore, should be drawn strictly on the differences between these

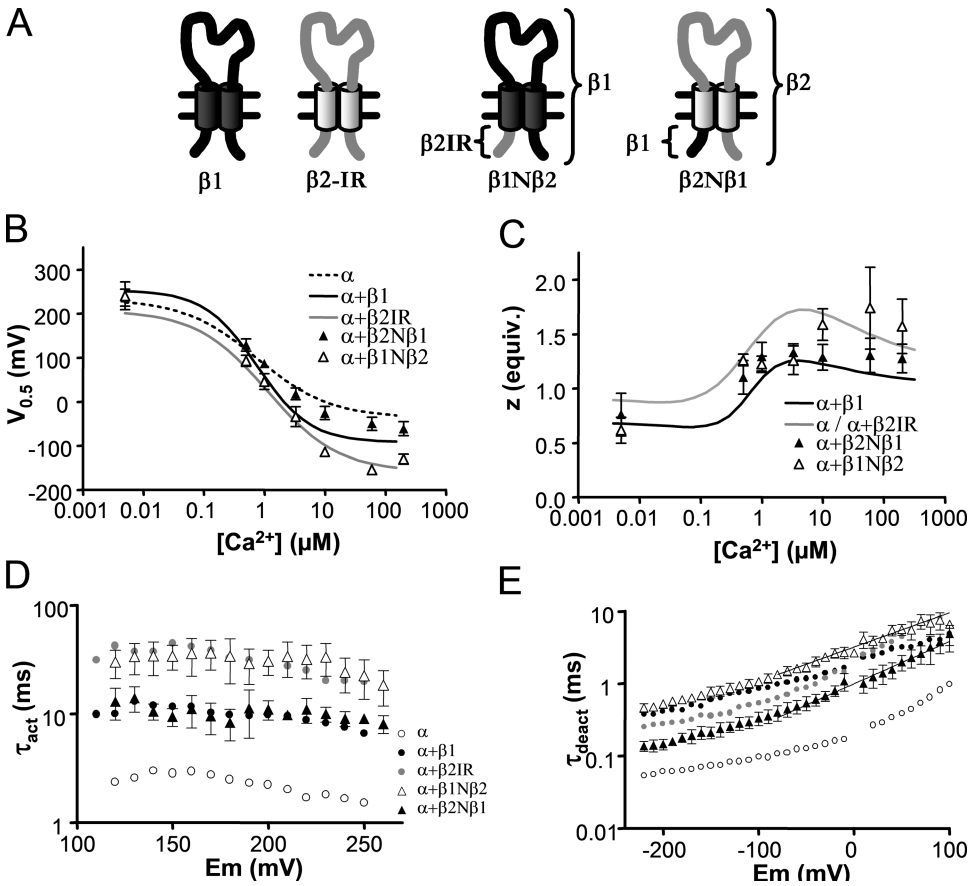

Figure 9. Activation parameters for α + β1Nβ2 and α + β2Nβ1 channels. (A) Schematic description of the β1Nβ2 and β2Nβ1 chimeras. (B) Average of the obtained $V_{0.5}$ values plotted against calcium concentration. For α, α + β1, and α + β2IR, only the best fit sigmoid concentration–effect curve (see Fig. 1 C) is depicted. (C) Average of the obtained z values plotted against calcium concentration. For α, α + β1, and α + β2IR, only the best fit curve (see Fig. 1 D) is depicted. Error bars are SD, n = 4–6. Missing error bars are smaller than symbol size. (D) Activation time constant (τ_{act}) at 5 nM intracellular [Ca^{2+}] plotted against activation voltage. Symbols represent mean ± SD. n = 4–11. (E) Deactivation time constant (τ_{deact}) at 5 nM intracellular [Ca^{2+}] plotted against voltage. Symbols represent mean ± SD. n = 4–6. In the case of α, α + β1, and α + β2IR, only the mean is shown. Lines represent the best fit of a simple exponential function to the data between −50 and +60 mV, extrapolated from −80 to +100 mV. The exponential factors expressed as electronic charges (z = slope×RT/F) are α + β1Nβ2, 0.28 ± 0.01; α + β2Nβ1, 0.34 ± 0.01.

subunits. It is possible that most of the effects of both subunits reside in a common structural feature of the extracellular loop, while the intracellular and transmembrane domains would be responsible for the fine tuning of these effects giving to each subunit its own identity. Though this is an issue that will need experiments with the other β subunits to be categorically addressed, several facts make us think that these domains do much more than subtle changes to the activation properties of the BK channel. First, one of the differences between β1 and β2 subunits is not quantitative but qualitative: the voltage dependence of the channel is greatly impaired in the presence of the β1-subunit while it remains unaffected by the β2-subunit. At least, our present results map regions of the β1-subunit that must interact with either the voltage sensors of the channel or the domains that couple the voltage sensor activation with channel opening. Second, a thorough analysis of the effects of these subunits suggested the possibility that both β subunits enhance the apparent calcium sensitivity by different mechanisms (Orio and Latorre, 2005). In this case, the regions that we have mapped would be responsible for a different regulatory mechanism in each β-subunit. Finally, all the voltage and calcium sensitivity in the BK channel has been so far mapped to transmembrane and intracellular domains: the voltage sensor is in the S4 membrane–spanning helix (Diaz et al., 1998), all the postulated calcium binding sites are proposed to be intracellular (Schreiber and Salkoff, 1997; Schreiber et al., 1999; Bian et al., 2001; Bao et al., 2002, 2004; Xia et al., 2002, 2004), and the coupling mechanisms for both voltage and calcium activation have been mapped to intracellular regions as well (see below, Functional Coupling). Therefore we think unlikely that an important contribution to the modulation of calcium- and voltage-dependent activation mechanisms of the BK

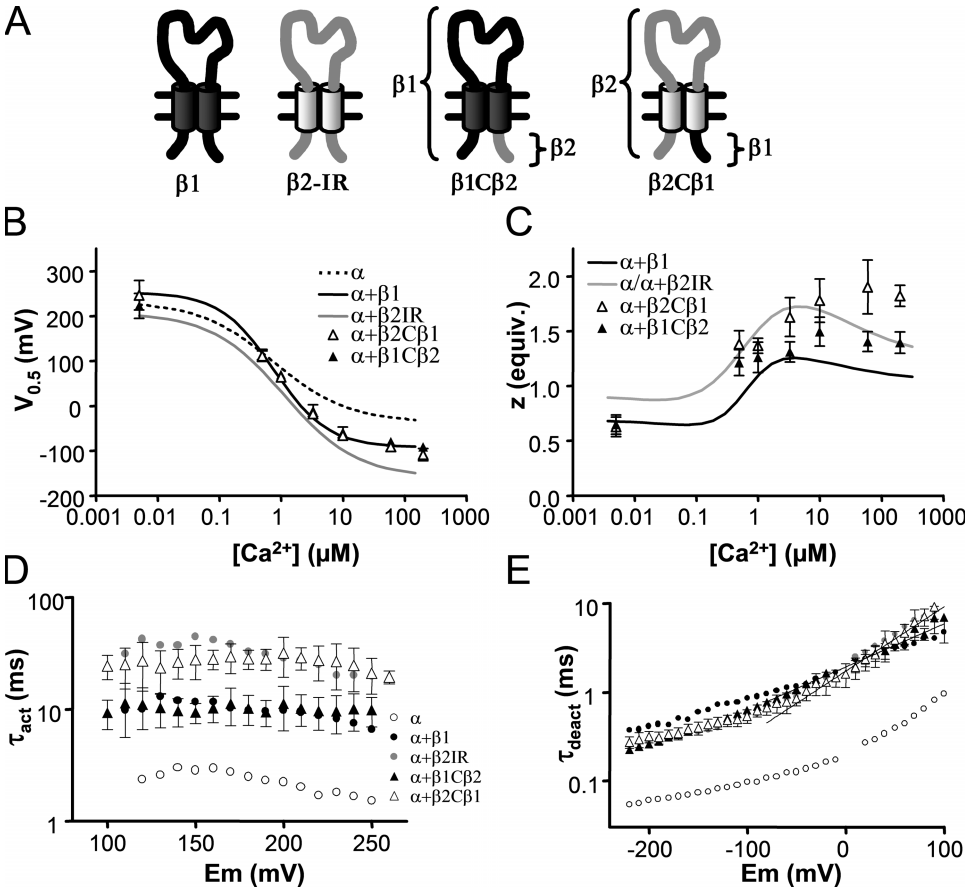

Figure 10. Activation parameters for α + β1Cβ2 and α + β2Cβ1 channels. (A) Schematic description of the β1Cβ2 and β2Cβ1 chimeras. (B) Average of the obtained $V_{0.5}$ values plotted against calcium concentration. For α, α + β1, and α + β2IR, only the best fit sigmoid concentration–effect curve (see Fig. 1 C) is depicted. (C) Average of the obtained z values plotted against calcium concentration. For α, α + β1, and α + β2IR, only the best fit curve (see Fig. 1 D) is depicted. Error bars are SD, n = 9–11. Missing error bars are smaller than symbol size. (D) Activation time constant (τ_{act}) at 5 nM intracellular [Ca^{2+}] plotted against activation voltage. Symbols represent mean ± SD. n = 8–12. (E) Deactivation time constant (τ_{deact}) at 5 nM intracellular [Ca^{2+}] plotted against voltage. Symbols represent mean ± SD. n = 4–8. In the case of α, α + β1, and α + β2IR, only the mean is shown. Lines represent the best fit of a simple exponential function to the data between −50 and +60 mV, extrapolated from −80 to +100 mV. The exponential factors expressed as electronic charges (z = slope×RT/F) are α + β1Cβ2, 0.29 ± 0.01; α + β2Cβ1, 0.43 ± 0.01.

channel may arise from an interaction of extracellular domains of β and α subunits.

Function of the Extracellular Region

Several roles have been attributed to the interaction between extracellular regions of the α and β subunits of the BK channel, all of them unrelated to changes in the voltage or calcium sensitivity of the channel. The external loop of β subunits plays an important role in determining ion permeation and the characteristics of toxin binding. The β4-subunit, for instance, induces a resistance of BK channels to CTX and IbTX block that is reproduced only by a chimera containing the loop of β4 (Meera et al., 2000). The β3-subunit produces an open channel rectification (Xia et al., 2000; Lingle et al., 2001; Zeng et al., 2001) that is dependent on the disulfide bridges in its extracellular region. Again, this effect is only reproduced by a chimera containing the extracellular loop of β3 (Zeng et al., 2003). In the case of the bovine β1-subunit, the adequate loop conformation appears to be a requisite for BK channel high affinity binding of CTX, as any of the four cysteines contained in the external β1 linker are critical in defining the ability of β1 in enhancing CTX binding (Hanner et al., 1998). Regarding the functional coupling between α and β1 subunits, the results that propose the extracellular domains as part of the interaction domain (Wallner et al., 1996) may be only of structural meaning, these domains being needed for the assembly of the heteromultimer rather than for functional coupling.

The present results add to this list of findings that the β-subunit external region may play only a minor role in the modulation of the calcium- and voltage-dependent activation mechanisms of the channel. This minor contribution cannot be excluded, though. We have recently shown that a point mutation in the extracellular loop of

the human β1-subunit modifies its effect on BK calcium sensitivity (Fernandez-Fernandez et al., 2004). Despite the physiological relevance of this effect, it is less than the differences between β1 and β2 subunits (e.g., at 500 nM calcium the E65K mutation induces a shift of 10 mV in $V_{0.5}$ while the difference between β1 and β2 subunits at 680 nM calcium is ∼20 mV), and this mutant still changes the channel kinetics the way the wild-type β1-subunit does. Thus, the extracellular loop may play a partial role in the modulation of apparent calcium sensitivity, possibly via some interaction with the external side of the voltage sensor (see Bao and Cox, 2005; Orio and Latorre, 2005).

Role of the Intracellular Termini

When only the intracellular and transmembrane regions are dissociated (NC and TMs chimeras) the resulting chimeras induce changes in channel properties that resemble the donor of the intracellular regions, suggesting that the intracellular ends are responsible for most of the functional coupling between α and β subunits. However in this case the results were not as clean as with the L chimeras, suggesting a shared role with the transmembrane regions in the modulation of channel properties. Interestingly, the β1NCβ2 and β2TMsβ1 chimeras (both having the NH_2 and COOH termini of β2) showed an enhanced effect on BK channel's calcium sensitivity, promoting a $V_{0.5}$ shift higher than that promoted by the β2IR-subunit.

Chimeras with only the NH_2 terminus exchanged (β1Nβ2 and β2Nβ1) showed a mixed behavior; however, there were important characteristics similar to the β-subunit contributing to the NH_2 terminus. In particular, the NH_2 terminus suffices to determine the BK channel activation kinetics and the behavior of z as a function of the Ca^{2+} concentration. A different result was obtained with the chimeras with only the COOH terminus exchanged (β1Cβ2 and β2Cβ1); in which there were minor differences in behavior compared with the parental β subunits. Thus, the NH_2 terminus of the β subunits is the most important structural determinant in the differences of modulation of the α-subunit by its auxiliary β1 and β2 subunits.

This finding is not surprising when other evidences are considered. In the case of β4-subunit, phosphorylation of its NH_2 and COOH termini is crucial for the functional coupling with the α-subunit (Jin et al., 2002). The addition of the phosphatase inhibitor okadaic acid (OA) eliminates the effect of coexpression of β4 subunits, indicating that phosphorylation of β4 eliminates its modulatory effects. This shows that the relevance of the intracellular ends of the β subunits in the α–β subunit coupling may be a characteristic of all β subunits. The NH_2 terminus of β2-subunit has a conserved cAMP, cGMP-dependent phosphorylation site (sequence KRKT), and its relevance for modulation of channel properties remains unknown.

Functional Coupling

It has been proposed that the intracellular domains of each BK α-subunit contributes two RCK (regulatory of K^+ conductance) domains and that these eight RCK domains form a gating ring similar to the gating ring of MthK channels (Jiang et al., 2001, 2002). The free energy provided by Ca^{2+} binding to the gating ring (chemical energy) is transformed in mechanical energy used to open the pore. The linker between the sixth (S6) transmembrane domain and the first RCK domain of the BK channel has also been shown to play a role in this molecular coupling, acting as a passive spring (Niu et al., 2004). In the case of the molecular coupling between voltage sensor activation and channel opening, the S4–S5 linker as well as the COOH- terminal half of the S6 segment have been postulated to play this role in other voltage-gated channels (Chen et al., 2001; Lu et al., 2002; Tristani-Firouzi et al., 2002).

It appears, therefore, inescapable that the intracellular domains of the BK channel are the most probable site of interaction for the modulation of the calcium and voltage sensitivity. Indeed, Qian et al. (2002) showed that the β1-subunit cannot enhance the calcium sensitivity of BK channels when the intracellular "tail" domain is replaced with the tail from the highly related, pH-dependent, Slo3 channel. The only effect of the β1-subunit that can be detected on this channel is a reduction of the voltage dependence as it does for the wt channel in the absence of calcium. This and other observations were interpreted as the β1-subunit interacting with the intracellular calcium-sensing machinery of the BK channel. We show here that the intracellular domains of the β1 and β2 subunits are indeed responsible for most of the channel activity modulation. An attractive hypothesis would be that the cytoplasmic regions of the β subunits interacts directly with the linker-gating ring complex, modifying the allosteric coupling factors involved in channel opening.

We thank Dr. Osvaldo Alvarez for helpful discussion, Dr. Eduardo Rosenmman and Luisa Soto for help in molecular biology, and the members of Latorre Laboratory for discussion of this work.

This work was supported by grants from the Fondo Nacional de Investigación Científica y Tecnológica (FONDECYT 103-0830 to R. Latorre, 200-0061 to P. Orio, and 201-0006 to P. Rojas), the Human Frontiers in Science Program (R. Latorre, M.A. Valverde, and L. Toro), National Institutes of Health (HL54970 to L. Toro), and Red HERACLES (FIS, Spain, to M.A. Valverde). During part of this work, P. Orio was recipient of a Ph.D. fellowship from Fundación Andes. The Centro de Estudios Cientificos is a Millenium Institute and is funded in part by a grant from Fundacion Andes.

Olaf S. Andersen served as editor.

Submitted: 26 July 2005
Accepted: 13 January 2006

REFERENCES

Bao, L., and D.H. Cox. 2005. Gating and ionic currents reveal how the BKCa channel's Ca^{2+} sensitivity is enhanced by its β1 subunit. *J. Gen. Physiol.* 126:393–412.

Bao, L., A.M. Rapin, E.C. Holmstrand, and D.H. Cox. 2002. Elimination of the BK(Ca) channel's high-affinity Ca^{2+} sensitivity. *J. Gen. Physiol.* 120:173–189.

Bao, L., C. Kaldany, E.C. Holmstrand, and D.H. Cox. 2004. Mapping the BKCa channel's "Ca^{2+} bowl": side-chains essential for Ca^{2+} sensing. *J. Gen. Physiol.* 123:475–489.

Behrens, R., A. Nolting, F. Reimann, M. Schwarz, R. Waldschutz, and O. Pongs. 2000. hKCNMB3 and hKCNMB4, cloning and characterization of two members of the large-conductance calcium-activated potassium channel β subunit family. *FEBS Lett.* 474:99–106.

Bian, S., I. Favre, and E. Moczydlowski. 2001. Ca^{2+}-binding activity of a COOH-terminal fragment of the *Drosophila* BK channel involved in Ca^{2+}-dependent activation. *Proc. Natl. Acad. Sci. USA.* 98:4776–4781.

Brenner, R., T.J. Jegla, A. Wickenden, Y. Liu, and R.W. Aldrich. 2000. Cloning and functional characterization of novel large conductance calcium-activated potassium channel β subunits, hKCNMB3 and hKCNMB4. *J. Biol. Chem.* 275:6453–6461.

Chen, J., J.S. Mitcheson, M. Tristani-Firouzi, M. Lin, and M.C. Sanguinetti. 2001. The S4-S5 linker couples voltage sensing and activation of pacemaker channels. *Proc. Natl. Acad. Sci. USA.* 98:11277–11282.

Cox, D.H., and R.W. Aldrich. 2000. Role of the β1 subunit in large-conductance Ca^{2+}-activated K^+ channel gating energetics. Mechanisms of enhanced Ca^{2+} sensitivity. *J. Gen. Physiol.* 116:411–432.

Cox, D.H., J. Cui, and R.W. Aldrich. 1997. Allosteric gating of a large conductance Ca-activated K^+ channel. *J. Gen. Physiol.* 110:257–281.

Diaz, L., P. Meera, J. Amigo, E. Stefani, O. Alvarez, L. Toro, and R. Latorre. 1998. Role of the S4 segment in a voltage-dependent calcium-sensitive potassium (hSlo) channel. *J. Biol. Chem.* 273:32430–32436.

Dick, G.M., C.F. Rossow, S. Smirnov, B. Horowitz, and K.M. Sanders. 2001. Tamoxifen activates smooth muscle BK channels through the regulatory β1 subunit. *J. Biol. Chem.* 276:34594–34599.

Dworetzky, S.I., C.G. Boissard, J.T. Lum-Ragan, M.C. McKay, D.J. Post-Munson, J.T. Trojnacki, C.P. Chang, and V.K. Gribkoff. 1996. Phenotypic alteration of a human BK (hSlo) channel by hSlo β subunit coexpression: changes in blocker sensitivity, activation/relaxation and inactivation kinetics, and protein kinase A modulation. *J. Neurosci.* 16:4543–4550.

Fernandez-Fernandez, J.M., M. Tomas, E. Vazquez, P. Orio, R. Latorre, M. Senti, J. Marrugat, and M.A. Valverde. 2004. Gain-of-function mutation in the KCNMB1 potassium channel subunit is associated with low prevalence of diastolic hypertension. *J. Clin. Invest.* 113:1032–1039.

H anner, M., R. Vianna-Jorge, A. Kamassah, W.A. Schmalhofer, H.G. Knaus, G.J. Kaczorowski, and M.L. Garcia. 1998. The β subunit of the high conductance calcium-activated potassium channel. Identification of residues involved in charybdotoxin binding. *J. Biol. Chem.* 273:16289–16296.

Horrigan, F.T., and R.W. Aldrich. 2002. Coupling between voltage sensor activation, Ca^{2+} binding and channel opening in large conductance (BK) potassium channels. *J. Gen. Physiol.* 120:267–305.

Horton, R.M., Z.L. Cai, S.N. Ho, and L.R. Pease. 1990. Gene splicing by overlap extension: tailor-made genes using the polymerase chain reaction. *Biotechniques.* 8:528–535.

Jiang, Y., A. Pico, M. Cadene, B.T. Chait, and R. MacKinnon. 2001. Structure of the RCK domain from the *E. coli* K^+ channel and demonstration of its presence in the human BK channel. *Neuron.* 29:593–601.

Jiang, Y., A. Lee, J. Chen, M. Cadene, B.T. Chait, and R. MacKinnon. 2002. Crystal structure and mechanism of a calcium-gated potassium channel. *Nature.* 417:515–522.

Jiang, Z., M. Wallner, P. Meera, and L. Toro. 1999. Human and rodent MaxiK channel β-subunit genes: cloning and characterization. *Genomics.* 55:57–67.

Jin, P., T.M. Weiger, Y. Wu, and I.B. Levitan. 2002. Phosphorylation-dependent functional coupling of hSlo calcium-dependent potassium channel and its hβ4 subunit. *J. Biol. Chem.* 277:10014–10020.

Knaus, H.G., A. Eberhart, G.J. Kaczorowski, and M.L. Garcia. 1994a. Covalent attachment of charybdotoxin to the β-subunit of the high conductance Ca^{2+}-activated K^+ channel. Identification of the site of incorporation and implications for channel topology. *J. Biol. Chem.* 269:23336–23341.

Knaus, H.G., K. Folander, M. Garcia-Calvo, M.L. Garcia, G.J. Kaczorowski, M. Smith, and R. Swanson. 1994b. Primary sequence and immunological characterization of β-subunit of high conductance Ca^{2+}-activated K^+ channel from smooth muscle. *J. Biol. Chem.* 269:17274–17278.

Lingle, C.J., X.H. Zeng, J.P. Ding, and X.M. Xia. 2001. Inactivation of BK channels mediated by the NH_2 terminus of the β3b auxiliary subunit involves a two-step mechanism: possible separation of binding and blockade. *J. Gen. Physiol.* 117:583–606.

Lu, Z., A.M. Klem, and Y. Ramu. 2002. Coupling between voltage sensors and activation gate in voltage-gated K^+ channels. *J. Gen. Physiol.* 120:663–676.

McManus, O.B., and K.L. Magleby. 1991. Accounting for the Ca^{2+}-dependent kinetics of single large- conductance Ca^{2+}-activated K^+ channels in rat skeletal muscle. *J. Physiol.* 443:739–777.

McManus, O.B., L.M. Helms, L. Pallanck, B. Ganetzky, R. Swanson, and R.J. Leonard. 1995. Functional role of the β subunit of high conductance calcium-activated potassium channels. *Neuron.* 14:645–650.

Meech, R.W. 1978. Calcium-dependent potassium activation in nervous tissues. *Annu. Rev. Biophys. Bioeng.* 7:1–18.

Meera, P., M. Wallner, Z. Jiang, and L. Toro. 1996. A calcium switch for the functional coupling between alpha (hslo) and β subunits (Kv,cαβ) of maxi K channels. *FEBS Lett.* 385:127–128.

Meera, P., M. Wallner, M. Song, and L. Toro. 1997. Large conductance voltage- and calcium-dependent K^+ channel, a distinct member of voltage-dependent ion channels with seven N-terminal transmembrane segments (S0-S6), an extracellular N terminus, and an intracellular (S9-S10) C terminus. *Proc. Natl. Acad. Sci. USA.* 94:14066–14071.

Meera, P., M. Wallner, and L. Toro. 2000. A neuronal β subunit (KCNMB4) makes the large conductance, voltage- and Ca^{2+}-activated K^+ channel resistant to charybdotoxin and iberiotoxin. *Proc. Natl. Acad. Sci. USA.* 97:5562–5567.

Nimigean, C.M., and K.L. Magleby. 2000. Functional coupling of the β1 subunit to the large conductance Ca^{2+}-activated K^+ channel in the absence of Ca^{2+}. Increased Ca^{2+} sensitivity from a Ca^{2+}-independent mechanism. *J. Gen. Physiol.* 115:719–736.

Niu, X., X. Qian, and K.L. Magleby. 2004. Linker-gating ring complex as passive spring and Ca^{2+}-dependent machine for a voltage- and Ca^{2+}-activated potassium channel. *Neuron.* 42:745–756.

Orio, P., and R. Latorre. 2005. Differential Effects of β1 and β2 subunits on BK channel activity. *J. Gen. Physiol.* 125:395–411.

Orio, P., P. Rojas, G. Ferreira, and R. Latorre. 2002. New disguises for an old channel: maxiK channel β-subunits. *News Physiol. Sci.* 17:156–161.

Qian, X., C.M. Nimigean, X. Niu, B.L. Moss, and K.L. Magleby. 2002. Slo1 tail domains, but not the Ca^{2+} bowl, are required for the β1 subunit to increase the apparent Ca^{2+} sensitivity of BK channels. *J. Gen. Physiol.* 120:829–843.

Schreiber, M., and L. Salkoff. 1997. A novel calcium-sensing domain in the BK channel. *Biophys. J.* 73:1355–1363.

Schreiber, M., A. Yuan, and L. Salkoff. 1999. Transplantable sites confer calcium sensitivity to BK channels. *Nat. Neurosci.* 2:416–421.

Shen, K.Z., A. Lagrutta, N.W. Davies, N.B. Standen, J.P. Adelman, and R.A. North. 1994. Tetraethylammonium block of Slowpoke calcium-activated potassium channels expressed in *Xenopus* oocytes: evidence for tetrameric channel formation. *Pflugers Arch.* 426:440–445.

Stühmer, W., and A.B. Parekh. 1995. Electrophysiological recordings from *Xenopus* oocytes. *In* Single Channel Recording. B. Sakmann and E. Neher, editors. Plenum Press, New York. 341–356.

Toro, L., M. Wallner, P. Meera, and Y. Tanaka. 1998. Maxi-K(Ca), a unique member of the voltage-gated K channel superfamily. *News Physiol. Sci.* 13:112–117.

Tristani-Firouzi, M., J. Chen, and M.C. Sanguinetti. 2002. Interactions between S4-S5 linker and S6 transmembrane domain modulate gating of HERG K^+ channels. *J. Biol. Chem.* 277:18994–19000.

Uebele, V.N., A. Lagrutta, T. Wade, D.J. Figueroa, Y. Liu, E. McKenna, C.P. Austin, P.B. Bennett, and R. Swanson. 2000. Cloning and functional expression of two families of β-subunits of the large conductance calcium-activated K^+ channel. *J. Biol. Chem.* 275:23211–23218.

Valverde, M.A., P. Rojas, J. Amigo, D. Cosmelli, P. Orio, M.I. Bahamonde, G.E. Mann, C. Vergara, and R. Latorre. 1999. Acute activation of Maxi-K channels (hSlo) by estradiol binding to the β subunit. *Science.* 285:1929–1931.

Vergara, C., R. Latorre, N.V. Marrion, and J.P. Adelman. 1998. Calcium-activated potassium channels. *Curr. Opin. Neurobiol.* 8:321–329.

Wallner, M., P. Meera, M. Ottolia, G.J. Kaczorowski, R. Latorre, M.L. Garcia, E. Stefani, and L. Toro. 1995. Characterization of and modulation by a β-subunit of a human maxi KCa channel cloned from myometrium. *Receptors Channels.* 3:185–199.

Wallner, M., P. Meera, and L. Toro. 1996. Determinant for β-subunit regulation in high-conductance voltage- activated and Ca^{2+}-sensitive K^+ channels: an additional transmembrane region at the N terminus. *Proc. Natl. Acad. Sci. USA.* 93:14922–14927.

Wallner, M., P. Meera, and L. Toro. 1999. Molecular basis of fast inactivation in voltage and Ca^{2+}-activated K^+ channels: a transmembrane β-subunit homolog. *Proc. Natl. Acad. Sci. USA.* 96:4137–4142.

Xia, X.M., J.P. Ding, and C.J. Lingle. 1999. Molecular basis for the inactivation of Ca^{2+}- and voltage-dependent BK channels in adrenal chromaffin cells and rat insulinoma tumor cells. *J. Neurosci.* 19:5255–5264.

Xia, X.M., J.P. Ding, X.H. Zeng, K.L. Duan, and C.J. Lingle. 2000. Rectification and rapid activation at low Ca^{2+} of Ca^{2+}-activated, voltage-dependent BK currents: consequences of rapid inactivation by a novel β subunit. *J. Neurosci.* 20:4890–4903.

Xia, X.M., X. Zeng, and C.J. Lingle. 2002. Multiple regulatory sites in large-conductance calcium-activated potassium channels. *Nature.* 418:880–884.

Xia, X.M., X. Zhang, and C.J. Lingle. 2004. Ligand-dependent activation of Slo family channels is defined by interchangeable cytosolic domains. *J. Neurosci.* 24:5585–5591.

Zeng, X.H., J.P. Ding, X.M. Xia, and C.J. Lingle. 2001. Gating properties conferred on BK channels by the β3b auxiliary subunit in the absence of its NH_2 and COOH termini. *J. Gen. Physiol.* 117:607–628.

Zeng, X.H., X.M. Xia, and C.J. Lingle. 2003. Redox-sensitive extracellular gates formed by auxiliary β subunits of calcium-activated potassium channels. *Nat. Struct. Biol.* 10:448–454.